Liquid Crystals
Publication details, including instructions for authors and subscription information:
http://www.informaworld.com/smpp/title~content=t713926090

Invited Lecture. Material properties, structural relations with molecular ensembles and electro-optical performance of new bicyclohexane liquid crystals in field-effect liquid crystal displays

Martin Schadt[a]; Richard Buchecker[a]; Klaus Müller[a]
[a] Central Research Units, F. Hoffmann-La Roche & Co. Ltd, Basel, Switzerland

To cite this Article Schadt, Martin , Buchecker, Richard and Müller, Klaus(1989) 'Invited Lecture. Material properties, structural relations with molecular ensembles and electro-optical performance of new bicyclohexane liquid crystals in field-effect liquid crystal displays', Liquid Crystals, 5: 1, 293 — 312

To link to this Article: DOI: 10.1080/02678298908026371

URL: http://dx.doi.org/10.1080/02678298908026371

Liquid Crystals, 1989, Vol. 5, No. 1, 293–312

Invited Lecture

Material properties, structural relations with molecular ensembles and electro-optical performance of new bicyclohexane liquid crystals in field-effect liquid crystal displays

by MARTIN SCHADT, RICHARD BUCHECKER and KLAUS MÜLLER
Central Research Units, F. Hoffmann-La Roche & Co. Ltd,
CH-4002 Basel, Switzerland

Several new classes of polar and non-polar bicyclohexane liquid crystals comprising alkenyl side chains are presented. The compounds exhibit low optical anisotropies, Δn, $< 0{\cdot}1$ and rotational viscosities, γ_1, as low as 35 cP at 22°C. This leads, in combination with large elastic expressions $\kappa = k_1 + (k_3 - 2k_2)/4 > 12 \times 10^{-12}$ N, to low viscoelastic ratios γ_1/κ and to short response times in field-effect liquid crystal displays (LCDs). Strong odd–even effects occur in the bend/splay elastic ratio k_3/k_1 upon shifting the alkenyl double bond from even into odd side chain positions. As a result the ratio k_3/k_1 can be tuned over the wide range $0{\cdot}9 \lesssim k_3/k_1 \lesssim 3{\cdot}0$. Correlations between the electro-optical properties of twisted nematic, supertwisted nematic, optical mode interference LCDs and material parameters demonstrate the high degree of multiplexability of the new compounds. Roche interactive molecular modelling is applied to determine the possible equilibrium configuration not only of single molecules, but for the first time to whole molecular ensembles comprising 12 molecules. First results show that the shape of the ensembles, E, depends on the position of the double bond in the side chains of the molecules. The length/width ratio of E decreases for even double bond positions.

1. Introduction

The rapid development of liquid crystal display (LCD) technology since the early 1970s is closely linked to the progress made in liquid crystal material research. With increasing complexity and diversity of the technology the demand for even more sophisticated liquid crystals has increased. To exploit the potential of the technology fully, to open up new applications and to improve the basic understanding of liquid-crystalline behaviour, new liquid crystals are required which possess as wide a bandwidth of material properties as possible. Prerequisites for the attainment of the goals are experimental techniques to investigate and correlate the relevant material and electro-optical properties with molecular structural elements. Attempts can then be made to establish molecular design criteria to find new and applicable materials.

Besides being greatly interested in liquid crystals with fast responses for virtually all display applications, we would like to combine, especially for the recently developed high information content LCDs, fast response *and* low optical anisotropy $\Delta n = (n_e - n_0)$ with the possibility of tuning the elastic properties to the requirements of the specific electro-optical effect used in the LCD. For example, in thin film transistor (TFT) [1] addressed twisted nematic (TN)-LCDs [2] for colour TV screens, the desired wide viewing angles and large number of gray levels can be achieved if the

TN-LCD is operated in its first transmission minimum [3]. This requires fast liquid crystals with a low birefringence. For the recently developed supertwist (STN)-LCD [4] and optical mode interference (OMI)-LCD [5] the liquid crystal materials must, in addition, exhibit large bend/splay elastic ratios if the desired high degree of multiplexability is to be achieved [5, 6].

So far there are only a few liquid crystal classes described in the literature which exhibit a low birefringence and whose rigid core consists of two cyclohexane rings. All of these possess saturated side chains [7–10]. The non-polar representatives among them, that is, the directly linked [9], as well as the ester [7] and the ethane [10] linked, bicyclohexanes exhibit pronounced smectic B phases which strongly diminish their applicability in nematic mixtures. Moreover, the large viscosities of the esters do not render them applicable for rapidly responding LCDs. For these reasons as well as for the experimental difficulties which result from the very low diamagnetic anisotropy of bicyclohexane cores, there are, except for standard phase transition data and for the cyano component CCH-7 [8], virtually no material properties of bicyclohexane liquid crystals published.

In our earlier work on phenylcyclohexane alkenyls [11–13] we have shown that the introduction of a double bond at specific side chain positions markedly affects the material properties of liquid crystals, especially the elastic constants and the viscosity. From our previous findings a number of questions arose, such as: (*a*) to what extent would alkenylation at different positions of side chains attached to bicyclohexane rigid cores lead to nematic properties; (*b*) whether odd–even effects of the material properties would result, similar to those which we had found for phenylcyclohexanes; (*c*) whether the new molecules could be designed such that low birefringence nematic liquid crystals with a wide bandwidth of material properties result; and (*d*) whether interactive molecular graphics modelling techniques could be applied not only to individual molecules, but to whole ensembles of molecules such that some of the unique elastic properties of liquid crystals could be related at least semiqualitatively with the ensemble?

Here we introduce a number of new, polar as well as non-polar bicyclohexane liquid crystal classes which exhibit pronounced nematic mesophases. Their optical, dielectric, viscous and some electro-optical properties, as well as all bulk elastic constants, are presented. The classes differ from each other with respect to the systematic changes made in the position of the alkenyl double bond in their side chains and/or with respect to their polar or non-polar substituents. The low viscoelastic ratios of the new compounds are shown to lead to short response times in LCDs. Moreover, seemingly small steric changes which result from shifting a double bond from odd into even positions are shown to affect markedly the overall dimensions of possible equilibrium configurations of ensembles of alkenyl molecules.

2. New alkenyl liquid crystals

2.1. *Polar (cyano) alkenyls*

The upper part of table 1 shows the structures of the new cyano alkenyl components which exhibit surprisingly wide nematic ranges and high nematic–isotropic transition temperatures T_{NI}. The nomenclature used is analogous to that introduced in [11]: alkenyl double bond is d_x, where the index designates the position of the bond from the nearest core ring, that is, from cyclohexane ring C (or phenyl ring P). The numbers in front of d_x are those of the carbon atoms attached to d_x. Included in

Table 1. Single components and binary mixtures **M1–M6** of cyano-bicyclohexane alkenyls. Except for $2d_1$CC and $0d_4$CC, which exhibit smectic B phases, all mesophases are nematic. T_m, melting temperature; T_{NI}, nematic–isotropic transition temperature.

Nomenclature	Structure	T_m/°C,	T_{sN}/°C,	T_{NI}/°C
$0d_1$CC	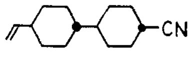	55·7		59·0
$1d_1$CC	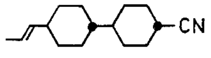	64·9		99·7
$2d_1$CC	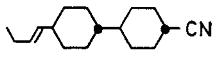	38·5	58	90·2
$3d_1$CC	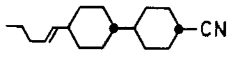	59·3		91·7
$0d_3$CC	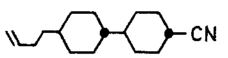	50·7		79·8
$1d_3$CC	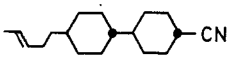	79·4		99·7
$0d_4$CC	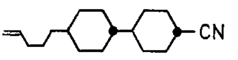	20·1	37	54·7
3CPO$d_3$1	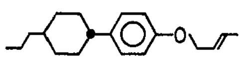	42·4		57·5
M1 = ($3d_1$CC, 3CPO$d_3$1) (50 : 50 mol %)		20		61·4
M2 = ($1d_3$CC, 3CPO$d_3$1) (50 : 50 mol %)		20		66·5
M3 = ($0d_4$CC, 3CPO$d_3$1) (50 : 50 mol %)		20		43·9
M4 = ($0d_1$CC, 3CPO$d_3$1) (50 : 50 mol %)		20		43·0
M5 = ($1d_1$CC, 3CPO$d_3$1) (50 : 50 mol %)		20		61·0
M6 = ($0d_3$CC, 3CPO$d_3$1) (50 : 50 mol %)		20		55·0

Table 1 is the non-polar, low viscous phenylcyclohexane compound 3CPO$d_3$1 [12] used in the binary mixtures **M1–M6** (see table 1): (*a*) to extend the mesomorphic range, thus allowing viscosity measurements down to room temperature; (*b*) to increase the diamagnetic anisotropy of the samples to be investigated such that they can be aligned in magnetic fields; and (*c*) to investigate the changes of material properties when combining polar with non-polar components.

To exclude possible changes of material properties due to different chain lengths, the positional influence of the alkenyl double bond was investigated in $3d_1$CC, $1d_3$CC and $0d_4$CC, where $R = C_5H_9$ = constant (see table 1). The homologous series $0d_1$CC, $1d_1$CC, $2d_1$CC and $3d_1$CC allows changes of material properties due to chain length variations to be investigated (see table 1).

2.2. *Non-polar alkenyls*

Table 2 shows the new non-polar alkenyl-alkoxy and alkyl-alkenyloxy bicyclohexanes which exhibit, except for $0d_4$CCO2, purely nematic mesophases. Like their polar counterparts (see table 1) their diamagnetic anisotropy $\Delta\chi$ is virtually zero. Therefore, and because of their simultaneously very small dielectric anisotropy $\Delta\varepsilon \approx 0$, the pure, non-polar bicyclohexanes in table 2 can be aligned neither in

Table 2. Single non-polar alkenyl and alkenyloxy bicyclohexane components and binary mixtures **M7–M12**. Except for the smectic B phase of 0d_4CCO2 all components and mixtures are nematic.

Nomenclature	Structure	T_m/°C	T_{sN}/°C	T_{NI}/°C
0d_3CCO2	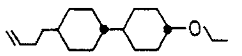	13·1		45·3
1d_3CCO2	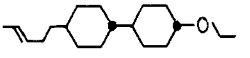	43·0		75·3
0d_4CCO2	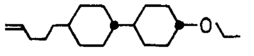	10·5	S_B	43·0
3CCO$d_3$0	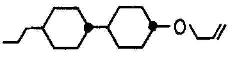	19·1		37·7
1d_3CCO1	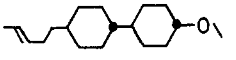	16·6		44·0
1d_3CPO2	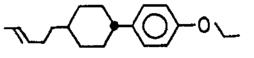	49·4		61·8
M7 = (0d_3CCO2, 3CPO$d_3$1) (50 : 50 mol %)		< 15		44·5
M8 = (1d_3CCO2, 3CPO$d_3$1) (50 : 50 mol %)		< 15		58·6
M9 = (0d_4CCO2, 3CPO$d_3$1) (50 : 50 mol %)		< 15		37·6
M10 = (3CCO$d_3$0, 3CPO$d_3$1) (50 : 50 mol %)		< 15		42·6
M11 = (1d_3CCO1, 3CPO$d_3$1) (50 : 50 mol %)		< 15		45·0
M12 = (0d_3CCO2, 1d_3CPO2) (50 : 50 mol %)		< 15		48·2

usual magnetic, nor in electric, fields. The investigation of those material properties that require field alignment is therefore only possible if either $\Delta\varepsilon$ or $\Delta\chi$ is increased. We have chosen to increase $\Delta\chi$ by combining the bicyclohexane components in the binary mixtures **M7–M12** in table 2 with the low viscous, non-polar phenylcyclohexanes 3CPO$d_3$1 or 1d_3CPO2 [12].

The bicyclohexane components listed in table 2 were designed such that wide nematic ranges, low viscoelastic properties and low birefringence results. In the following, the influence of different double bond positions on the material properties of the non-polar mixtures in table 2 are best seem from comparisons between **M8** and **M9**. Comparisons between **M7**, **M8** and **M11** will show the influence of changes due to the chain length variations. **M10** comprises an alkyl-alkenyloxy bicyclohexane; whereas **M7** and **M12** allow comparisons between the two different phenylcyclohexanes 3CPO$d_3$1 and 1d_3CPO2 (see tables 1 and 2).

3. Experimental techniques

The static *dielectric constants* $\varepsilon_\perp$ and $\varepsilon_\parallel$ of the binary mixtures **M1–M12** were determined from the complex impedance of a parallel plate capacitor comprising the magnetic field-aligned mixtures ($\Delta\chi > 0$) as a dielectric [14]. For single bicyclohexane components, where $\Delta\chi \approx 0$, magnetic field alignment of the nematic director is not possible. In these cases surface aligned samples were prepared with homogeneous and homeotropic wall alignment. The quality of the homeotropically aligned samples, from which $\varepsilon_\parallel$ was determined, was checked conoscopically. To ensure low bias tilt angles ($<1°$) in parallel aligned LC layers, angular evaporated SiO_x boundaries were used [15].

The *bulk viscosity* η was determined with a rotating-cone Brookfield microviscometer [14]. The *refractive indices* n_0 and n_e were measured at the wavelength $\lambda = 520\,nm$ in an Abbé refractometer using a homogeneously surface aligned prism.

For diamagnetically positive anisotropic mixtures **M1–M12** the splay (k_{11}), twist (k_{22}) and bend (k_{33}) *elastic constants* were determined in surface aligned (parallel) samples. Deformation of the nematic director $\hat{\mathbf{n}}$ was induced by a magnetic field, and the director deformation was monitored optically [16].

For the positive dielectric anisotropic cyanobicyclohexanes Xd_YCC electric field-induced deformation instead of magnetic deflection of $\hat{\mathbf{n}}$ was used. From the optically monitored deformation, k_{11} and k_{33} follow [14, 16]. Since $\Delta\chi \approx 0$ the twist elastic constant k_{22} could not be determined in the same parallel aligned samples that were used to determine k_{11} and k_{33}; i.e. from the threshold of the magnetic field-induced twist deformation [16]. Instead, k_{22} was determined via the capacitive threshold voltage V_c of a twist cell from [2, 14]:

$$\begin{aligned} V_c &= \pi\left(\frac{k_{11} + (k_{33} - 2k_{22})/4}{\varepsilon_0 \Delta\varepsilon}\right)^{1/2} \\ &= \pi\left(\frac{K}{\varepsilon_0 \Delta\varepsilon}\right)^{1/2} \end{aligned} \tag{1}$$

Because the dielectric displacement D is independent of the coordinate z normal to the cell surface only in non-conducting liquid crystal samples, electric field-induced director deformations can lead to large errors in elastic experiments if the samples are conducting [16, 17]. However, we have shown [16] that the inevitable conduction problem which is most pronounced at high temperatures can be overcome when using highly purified liquid crystals. The conditions

$$\frac{\sigma_\perp \Delta\sigma}{\varepsilon_\perp \Delta\varepsilon (\omega\varepsilon_0)^2} \ll 1 \quad \text{and} \quad \left(\frac{\sigma_\perp}{\varepsilon_\perp \omega\varepsilon_0}\right)^2 \ll 1 \tag{2}$$

have to be fulfilled, where $\boldsymbol{\sigma}$ is the conductivity tensor and ω is the angular frequency of the electric field. With $\omega = 10{\cdot}05\,kHz$ and typical conductivities of $\Delta\sigma < \sigma_\perp = 10^{-8}\,\Omega\,cm^{-1}$ and $\Delta\varepsilon \approx \varepsilon_\perp \approx 4$ at $T = (T_{NI} - 10°C)$, requirements (2) were met in our experiments.

The *rotational viscosity* γ_1 was determined from the small angle relaxation of the nematic direction $\hat{\mathbf{n}}$ caused by a small pulsed magnetic field that was applied perpendicular to a main permanent alignment field $\hat{\mathbf{H}}_0$ [18 (a)]. The director relaxation was monitored via the corresponding change of capacitance of the nematic layer. Because of the required magnetic field alignment of the samples, the γ_1 experiments were restricted to the binary mixtures **M1–M12**.

The static and dynamic *electro-optical performance* of mixtures **M1–M6** ($\Delta\varepsilon > 0$) was investigated in transmissive TN-LCDs. Collimated white light at vertical incidence and $d = 8\,\mu m$ electrode gaps were used. The response times t_{on} and t_{off} correspond to the respective transmission changes 10 to 90 per cent and 100 to 10 per cent which result from applying the (temperature dependent) gated square wave driving voltage $V(T) = 2{\cdot}5 \times V_{10}(T)$; where V_{10} is the optical threshold voltage at 10 per cent transmission [14, 18].

4. Performance of bicyclohexane alkenyls

4.1. *Cyano alkenyls*

Figure 1 shows the temperature dependence of the splay (k_{11}), twist (k_{22}) and bend (k_{33}) elastic constants of the cyano bicyclohexane alkenyl components Yd_xCC (see table 1). From figure 1 it is apparent that k_{33} is most affected by the position of the alkenyl bond. Thus, already at the high temperature end, at $T/T_{NI} = 0{\cdot}95$, where the differences are smallest, the large ratio $k_3(1d_3CC)/k_3(0d_4CC) = 2{\cdot}7$ results. Since both $1d_3CC$ and $0d_4CC$ have the same length side chain, the large difference in k_3 can be due only to the different positions of the double bonds. The respective twist and splay ratios which follow from figure 1 are much smaller, namely 1·7 and 1·5.

From figure 1 it also follows that the bend elastic constants of the homologous alkenyls $1d_1CC$, $2d_1CC$, and $3d_1CC$ decrease strongly with increasing chain length.

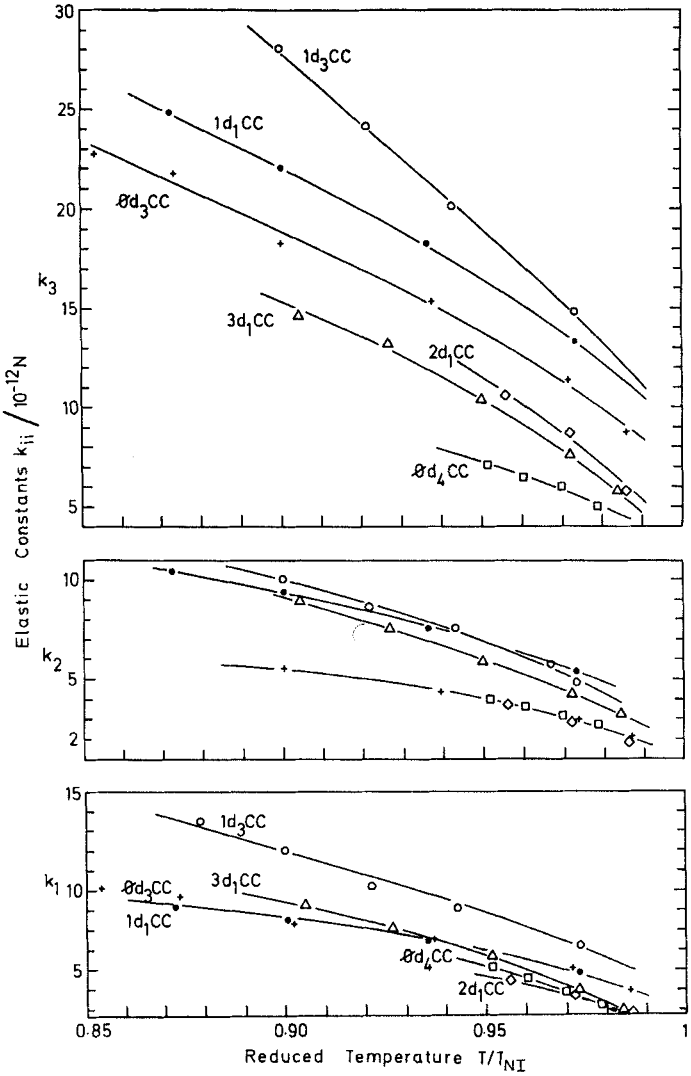

Figure 1. Temperature dependence of the splay (k_1), twist (k_2) and bend (k_3) elastic constants of the cyano-bicyclohexane alkenyls Yd_xCC (see table 1).

This finding corresponds with the trends reported for other homologous liquid crystal classes with saturated side chains [19].

As we will show, the elastic ratios k_3/k_1 and k_2/k_1 strongly affect the electro-optical performance of LCDs. Therefore, the elastic ratios k_2/k_1 and k_3/k_1 which follow from figure 1 are shown separately in figure 2. Comparing 3d_1CC, 1d_3CC and 0d_4CC in figure 2 shows that k_3/k_1 increases strongly when shifting the double bond from position 1 to position 3, whereas a strong decrease occurs for shifts between 3 to 4 and 1 to 4. This result shows that the bend/splay elastic ratios of the new cyano bicyclohexane alkenyls exhibit the same odd–even behaviour which we first found in cyano phenylcyclohexane alkenyls [11, 13]: odd double bond positions increase k_3/k_1 whereas even positions lead to a decrease. Moreover, figure 2 also shows the expected decrease of k_3/k_1 with increasing chain length within the homologous alkenyl series Yd_1CC. Moreover, from the upper part of figure 2 it follows that the twist/splay elastic ratio k_2/k_1 of cyano bicyclohexane alkenyls does not depend in an obvious way

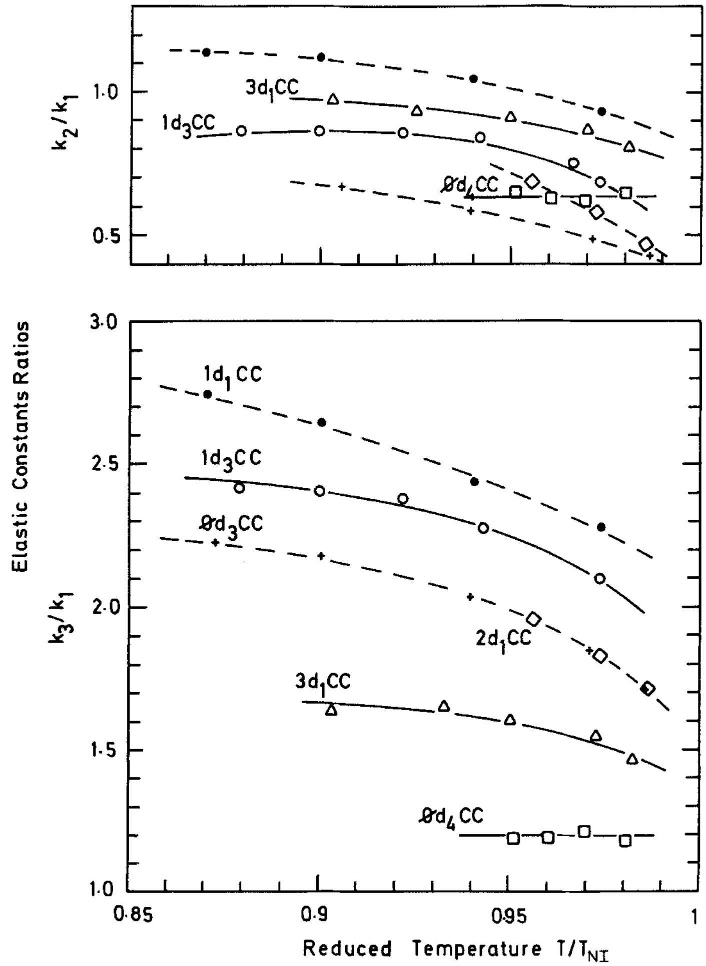

Figure 2. Temperature dependence of the elastic ratios bend/splay (k_3/k_1) and twist/splay (k_2/k_1) of cyano-bicyclohexane alkenyls Yd_xCC. The solid graphs belong to those alkenyls with the side chain $R = C_5H_{11}$ = constant (see table 1).

on the position of the double bond d_x. The variation of k_2/k_1 among different compounds are considerably smaller than that of k_3/k_1.

Table 3 summarizes the elastic, dielectric and optical properties of the cyano bicyclohexane alkenyls Yd_xCC. Also shown in table 3 are the material parameters of the binary mixtures **M1–M6** as well as those of the non-polar component 3CPO$d_3$1 used in mixtures **M1–M6**. The data in bold type were determined at the shifted temperatures $T = (T_{NI} - 10°C)$, whereas the others are room temperature data (22°C). From the elastic ratios k_3/k_1 at $(T_{NI} - 10°C)$ in table 3 it follows that k_3/k_1 for the (1 : 1 molar) mixtures **M1–M6** depends, approximately linearly, on k_3/k_1 of their components. The same applies to the dielectric and optical anisotropies. However, this does not hold for the elastic expression κ. Still, κ for the mixtures follows the trend of its components (see table 3). From the first three lines of the component data listed in table 3 it also follows that the dielectric, as well as the optical anisotropy exhibits the same positional dependence. That is, odd double bond positions lead to increased values of $\Delta\varepsilon$ and Δn, whereas a decrease results for even positions. This result, which is contradictory to the usual representation of alkenyl side chains (see tables 1 and 2), shows that the alignment of the π-electron $-C=C-$ double bonds are more parallel to the nematic director $\hat{n}$ in odd positions than in even positions. These findings agree with our earlier results for phenylcyclohexane alkenyls [11]. They are attributed to the specific steric conformations of alkenyl side chains which result if a cylindrically symmetric restriction of the spatial mobility of the chains in the nematic phase is assumed [12].

The left hand side of figure 3 shows the temperature dependence of the rotational viscosity γ_1 of mixtures **M1–M6**. From this it follows that $\gamma_1(T)$ can be described for $T \ll T_{NI}$ by

$$\gamma_1 \propto \exp(A/kT) \tag{3}$$

where A is an activation energy. Figure 3 shows that only small differences occur between the activation energies of different mixtures. Compared with γ_1 of other liquid crystals, including the phenylcyclohexanes [11–13], the low viscosities of all the mixtures in figure 3 are noteworthy. It is also interesting to compare their viscosities relative to the pure, low viscous non-polar alkenyl 3CPO$d_3$1. Despite their positive dielectric anisotropy which tends to increase γ_1, the short side chain cyano compound 0d_1CC, as well as the long side chain component 0d_4CC, further reduce γ_1 of 3CPO$d_3$1 (cf. mixtures **M4** and **M3**). Moreover, figure 3 shows a strong increase of γ_1(**M5**) compared with γ_1(**M4**). This demonstrates that increasing the chain length (of 0d_1CC) by just one methyl group may strongly affect the material properties, especially those of short side chain compounds.

The right hand side of figure 3 shows the temperature dependence of the viscoelastic ratio γ_1/κ and the turn-off times t_{off} of TN-LCDs comprising mixtures **M3–M6**. In a small angle approximation, which does not really hold for t_{off} in figure 3, the viscoelastic ratio determines the complex electro-optical response of TN-LCDs [11, 20]:

$$t_{off} \propto \gamma_1/\kappa, \qquad \kappa = k_{11} + (k_{33} - 2k_{22})/4. \tag{4}$$

From the right hand side of figure 3 it follows that the order of γ_1/κ for the different mixtures is not the same as their order for γ_1 on the left hand side of the figure. Thus, the viscoelastic ratio of the low viscous mixture **M3** is largest, whereas γ_1/κ of the most viscous mixture **M5** is smallest. The reversal of order is a result of the small κ value

Table 3. Splay (k_{11}), twist (k_{22}) and bend (k_{33}) elastic constants as well as $\kappa = [k_{11} + (k_{33} - 2k_{22})/4]$ of the cyano-bicyclohexane alkenyls Yd_xCC. Also included are the data for the binary mixtures **M1–M6** and for the phenylcyclohexane alkenyl 3CPO$d_3$1 (see table 1). The dielectric constants are: $\varepsilon_\perp$, $\Delta\varepsilon = (\varepsilon_\parallel - \varepsilon_\perp)$; the ordinary refractive index is n_0 and the optical anisotropy is $\Delta\nu = (n_e - n_0)$. The data in bold type were determined at the shifted temperature (T_{NI} − 10°C), whereas the others are room temperature data (22°C).

Liquid crystal	$k_{11}/10^{-12}$ N	$k_{22}/10^{-12}$ N	$k_{33}/10^{-12}$ N	κ	k_3/k_1	$\varepsilon_\perp$	$\Delta\varepsilon$	$\Delta\varepsilon/\varepsilon_\perp$	n_0	Δn
3d_1CC	**4·93**	**4·37**	**7·66**	**4·7**	**1·6**	**4·54**	**3·82**	**0·84**	**1·456**	**0·060**
1d_3CC	**7·00**	**4·80**	**14·6**	**8·2**	**2·1**	**4·12**	**4·61**	**1·12**	**1·456**	**0·065**
0d_4CC	**4·92**	**3·06**	**6·02**	**4·9**	**1·2**	**4·55**	**3·60**	**0·79**	**1·473**	**0·046**
1d_1CC	**5·83**	**5·40**	**13·4**	**6·5**	**2·3**	**4·35**	**5·03**	**1·16**	**1·457**	**0·066**
2d_1CC	**4·69**	**2·87**	**8·81**	**5·5**	**1·9**	**4·50**	**4·57**	**1·02**	**1·459**	**0·060**
0d_3CC	**6·11**	**2·99**	**11·4**	**7·4**	**1·9**	**4·12**	**4·48**	**1·09**	**1·467**	**0·056**
	10·7	7·10	24·3	13·2	2·3	3·60	5·18	1·44	1·477	0·074
M1 = (3d_1CC, 3CPO$d_3$1)	**5·92**	**3·84**	**8·29**	**6·0**	**1·4**	**3·81**	**2·77**	**0·73**	**1·477**	**0·071**
	10·0	6·39	15·6	10·7	1·6	3·69	3·25	0·88	1·483	0·090
M2 = (1d_3CC, 3CPO$d_3$1)	**6·45**	**4·32**	**10·6**	**6·9**	**1·6**	**3·74**	**2·88**	**0·77**	**1·475**	**0·074**
	11·7	7·94	22·0	13·2	1·9	3·62	3·53	0·97	1·484	0·094
M3 = (0d_4CC, 3CPO$d_3$1)	**5·29**	**3·23**	**6·50**	**5·3**	**1·2**	**4·00**	**2·30**	**0·57**	**1·485**	**0·064**
	7·33	4·42	9·20	7·4	1·3	3·92	2·60	0·66	1·486	0·074
M4 = (0d_1CC, 3CPO$d_3$1)	**5·60**	**3·34**	**8·53**	**6·1**	**1·5**	**4·01**	**2·67**	**0·66**	**1·485**	**0·071**
	7·17	4·01	11·7	8·1	1·6	3·94	3·03	0·77	1·487	0·081
M5 = (1d_1CC, 3CPO$d_3$1)	**6·52**	**3·73**	**10·9**	**7·4**	**1·7**	**3·84**	**3·10**	**0·81**	**1·478**	**0·077**
	10·1	5·27	19·6	12·4	1·9	3·72	3·76	1·01	1·485	0·095
M6 = (0d_3CC, 3CPO$d_3$1)	**6·02**	**4·26**	**9·04**	**6·1**	**1·5**	**3·82**	**2·55**	**0·67**	**1·480**	**0·070**
	9·35	6·60	15·7	10·0	1·7	3·71	3·04	0·82	1·485	0·086
3CPO$d_3$1	**10·9**	**5·60**	**12·4**	**11·2**	**1·14**	**3·06**	**−0·33**	**−0·11**	**1·486**	**0·090**

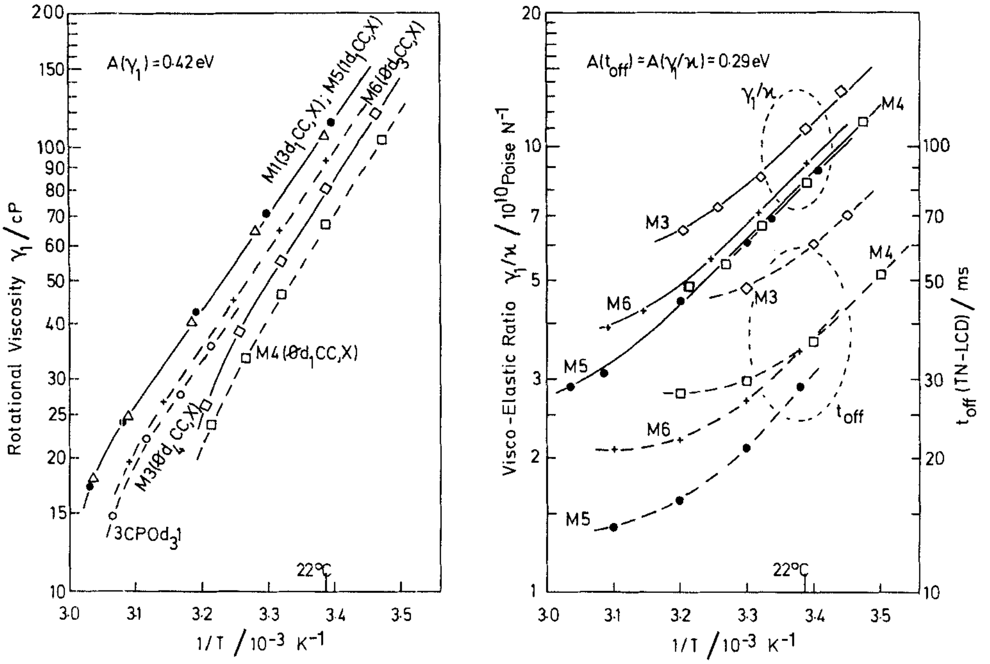

Figure 3. (Left) Temperature dependence of the rotational viscosity γ_1 for mixtures **M1**, **M3**–**M6** and of 3CPO$d_3$1. The abbreviation X = 3CPO$d_3$1 is used in the mixture composition. (Right) Temperature dependence of the viscoelastic ratio γ_1/κ and the turn-off time t_{off} for TN-LCDs with d = 8 μm electrode gap.

of the alkenyls with even double bond position [13] which the present compounds confirm (see table 3).

Comparing the response times t_{off} with γ_1/κ in figure 3 shows that the sequence of the t_{off} graphs exhibits the same, although more pronounced, order as the sequence of the γ_1/κ graphs. Moreover, the temperature dependence of t_{off} is comparable with that of γ_1/κ (cf. also $\gamma_1(T)$ in figure 3). Thus, the viscoelastic ratio γ_1/κ describes, at least qualitatively, the practical (100 to 10 per cent) turn-off times of TN-LCDs correctly. Therefore, the ratio γ_1/κ is a useful parameter for estimating the potential response behaviour of non-polar liquid crystals whose response cannot be measured directly because $\Delta\varepsilon \lesssim 0$.

Table 4 summarizes the bulk and rotational viscosities, the viscoelastic ratios γ_1/κ and the activation energies A of γ_1 for mixtures **M1**–**M6**. Also included in table 4 are the respective optical threshold voltages V_{10} and the response times of TN-LCDs.

4.2. *Non-polar alkenyls*

Figure 4 shows the temperature dependence of the bend elastic constant k_{33} as well as the elastic ratios k_{33}/k_{11} and k_{22}/k_{11} for the non-polar mixtures **M7**–**M12** given in table 2. Comparing the k_3 data and the elastic ratios k_3/k_1 for **M7**, **M8** and **M9** in figure 4 shows that non-polar alkenyls exhibit elastic odd–even effects analogous to those found previously. That is, odd double bond positions increase k_3 and k_1, especially when they are substituted by one methyl group (cf. **M7** and **M8**), whereas even positions strongly reduce these values (**M9**).

Table 4. Bulk viscosity η, rotational viscosity γ_1, viscoelastic ratio γ_1/κ and activation energy $A(\gamma_1)$ for mixtures **M1**–**M6** and of 3CPO$d_3$1. V_{10} is the optical threshold voltage of $d = 8\,\mu$m TN-LCDs; t_{on} and t_{off} are the TN-LCD response times. The data in bold type are (T_{NI} − 10°C) values, whereas the others are room temperature data (22°C).

Liquid crystal	η/cP	γ_1/cP	$\gamma_1/\kappa^{-1}\,10^{-12}\,m^{-2}\,s^{-1}$	$A(\gamma_1)$/eV	t_{on}/ms	t_{off}/ms	V_{10}/V
M1 = (3d_1CC, 3CPO$d_3$1)	**9**	**24**	**4.0**		**7**	**15**	**1·81**
	23	109	10	0·42	14	28	2·43
M2 = (1d_3CC, 3CPO$d_3$1)	**7**	–	–	–	**5**	**12**	**1·94**
	21†	–	–	–	13	23	2·68
M3 = (0d_4CC, 3CPO$d_3$1)	**14**	**39**	**7·3**		**13**	**32**	**1·74**
	22	80	11	0·46	18	43	1·99
M4 = (0d_1CC, 3CPO$d_3$1)	**13**	**33**	**5·4**		**9**	**21**	**1·75**
	19	67	8·2	0·46	13	27	1·95
M5 = (1d_1CC, 3CPO$d_3$1)	**7**	**24**	**3·2**		**6**	**12**	**1·85**
	21	105	8·5	0·42	12	22	2·48
M6 = (0d_3CC, 3CPO$d_3$1)	**9**	**27**	**4·3**		**7**	**16**	**1·89**
	19	93	9·2	0·44	13	25	2·36
3CPO$d_3$1	**5·3**	**22**	**1·9**		–	–	–
	13·5†	86	–	0.42	–	–	–

† Extrapolated values.

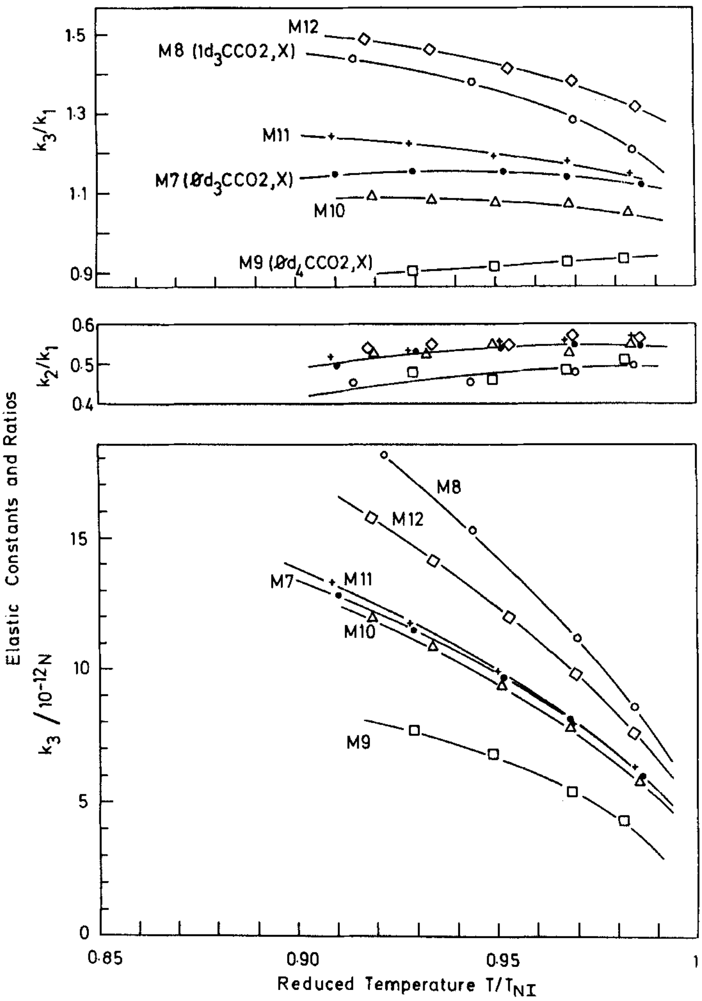

Figure 4. Temperature dependence of the elastic constants for the non-polar alkenyl mixtures **M7–M12** (see table 2). The abbreviation X = 3CPO$d_3$1 is used in the mixture compositon.

Table 5 shows the elastic, dielectric and optical properties for mixtures **M7–M12** as well as those for the phenylcyclohexane components 3CPO$d_3$1 and 1d_3CPO2 (see table 2). The data in bold type were determined at the shifted temperatures (T_{NI} − 10°C), the others are values at 22°C. It is interesting to note the large difference between the elastic ratios k_3/k_1 of 3CPO$d_3$1 and 1d_3CPO2 in table 5 which is also reflected in mixtures **M7** and **M12**. The difference is astonishing because both compounds exhibit odd double bond side chains. However, since the (saturated) alkyl chain of 3CPO$d_3$1 is attached to C, whereas the saturated side chain of 1d_3CPO2 comprises an oxygen and is attached to P, the different ratios are not necessarily due to the alkenyloxy side chain of 3CPO$d_3$1 only (cf. also k_{ii} for **M8** and **M11** in table 5). These examaples illustrate, again [11, 18], that small structural changes, such as those made close to the rigid core of the molecules, may markedly affect the material properties of liquid crystals.

Figure 5 shows the temperature dependence of the rotational viscosity γ_1 and the viscoelastic ratio γ_1/κ of the non-polar mixtures **M7–M12** (see table 2). A summary

Table 5. Elastic, dielectric and optical material constants for non-polar bicyclohexane alkenyl mixtures **M7–M12** (see table 2) and for the phenylcyclohexane alkenyls 3CPO$d_3$1 and 1d_3CPO2. The data in bold type were determined at the shifted temperature (T_{NI} − 10°C), whereas the others are room temperature data (22°C).

Liquid crystal	$k_{11}/10^{-12}$N	$k_{22}/10^{-12}$N	$k_{33}/10^{-12}$N	κ	k_3/k_1	$\varepsilon_\perp$	$\Delta\varepsilon$	n_0	Δn
M7 = (0d_3CCO2, 3CPO$d_3$1)	**7·07**	**3·78**	**8·08**	**7·2**	**1·1**	**3·05**	**−0·31**	**1·479**	**0·065**
	10·1	5·25	11·6	10·3	1·1	3·13	−0·38	1·482	0·074
M8 = (1d_3CCO2, 3CPO$d_3$1)	**8·71**	**4·13**	**11·2**	**9·4**	**1·3**	**2·96**	**−0·21**	**1·473**	**0·070**
	15·2	6·8	21·8	17·0	1·5	3·09	−0·29	1·481	0·086
M9 = (0d_4CCO2, 3CPO$d_3$1)	**5·89**	**2·82**	**5·46**	**5·8**	**0·9**	**3·06**	**−0·31**	**1·482**	**0·060**
	7·41	3·40	6·77	7·4	0·9	3·10	−0·35	1·483	0·066
M10 = (3CCO$d_3$0, 3CPO$d_3$1)	**7·27**	**4·08**	**7·80**	**7·2**	**1·1**	**3·09**	**−0·15**	**1·482**	**0·064**
	10·0	5·60	10·8	9·9	1·1	3·15	−0·19	1·481	0·072
M11 = (1d_3CCO1, 3CPO$d_3$1)	**6·73**	**3·69**	**7·94**	**6·9**	**1·2**	**3·08**	**−0·20**	**1·482**	**0·066**
	9·64	5·23	11·8	9·9	1·2	3·16	−0·25	1·484	0·076
M12 = (0d_3CCO2, 1d_3CPO2)	**7·16**	**4·05**	**9·88**	**7·6**	**1·4**	**3·02**	**−0·31**	**1·477**	**0·068**
	10·6	5·71	15·8	11·7	1·5	3·11	−0·29	1·482	0·078
3CPO$d_3$1	**10·9**	**5·60**	**12·4**	**11·2**	**1·1**	**3·06**	**−0·33**	**1·486**	**0·090**
1d_3CPO2	**10·1**	**4·82**	**15·7**	**11·6**	**1·6**	**3·03**	**−0·27**	**1·483**	**0·095**

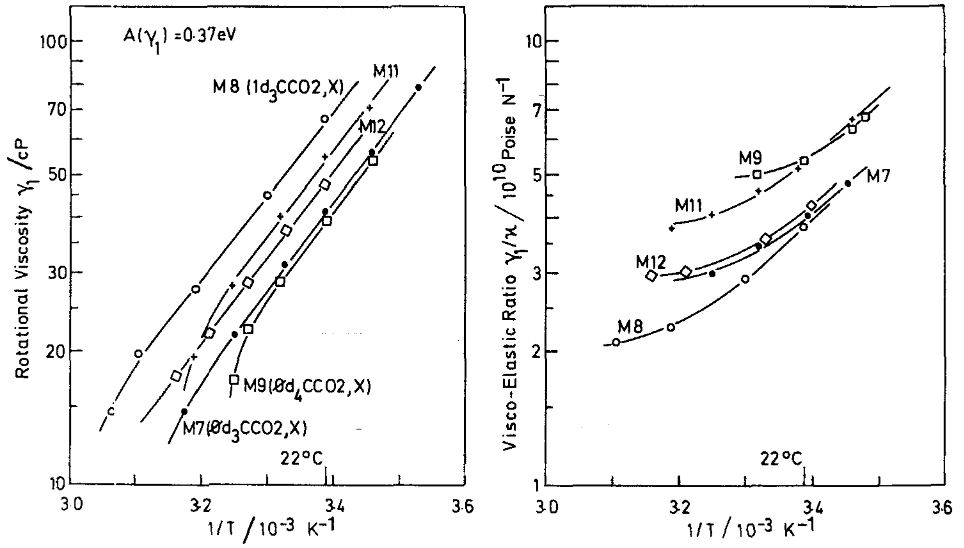

Figure 5. Temperature dependence of the rotational viscosity γ_1 and the viscoelastic ratio γ_1/κ for non-polar alkenyl mixtures **M7–M12** (see table 2). The abbreviation X = 3CPO$d_3$1 is used in the mixture composition.

Table 6. Rotational (γ_1) and bulk (η) viscosity, viscoelastic ratio γ_1/κ and activation energy $A(\gamma_1)$ for non-polar alkenyl mixtures **M7–M12** (see table 2).

Liquid crystal	η/cP	γ_1/cP	$\gamma_1\kappa^{-1}/10^{-12}\mathrm{m}^{-2}\mathrm{s}^{-1}$	$A(\gamma_1)$/eV
M7 = (0d_3CCO2, 3CPO$d_3$1)	**6·8**	**41**	**5·7**	
	10·3	62	6·0	0·37
M8 = (1d_3CCO2, 3CPO$d_3$1)	**5·2**	**20**	**3·0**	
	11·4	66	4·0	0·37
M9 = (0d_4CCO2, 3CPO$d_3$1)	**10·3**	**29**	**5·0**	
	12·4	39	5·3	0·37
M10 = (3CCO$d_3$0, 3CPO$d_3$1)	**7·1**	**22**	**3·0**	
	9·5	40	4·0	0·37
M11 = (1d_3CCO1, 3CPO$d_3$1)	**7·8**	**27**	**3·9**	
	11·7	53	5·4	0·37
M12 = (0d_3CCO2, 1d_3CPO2)	**6·3**	**22**	**2·9**	
	9·8	47	4·1	0·37
1d_3CPO2	**4·7**	**25**	**2·1**	

of the results, including bulk viscosity data, is given in table 6. From figure 5 it follows, as for the cyano compounds, that even double bond positions which lead to low κ values exhibit, despite their low rotational viscosities, large viscoelastic ratios, whereas the opposite holds for 3-alkenyls (cf. **M8** and **M9** in figure 5). Figure 5 also shows that the non-polar bicyclohexanes exhibit very low rotational viscosities. Some are, with γ_1(22°C) < 40 cP, less than half as viscous as the low viscosity phenyl-cyclohexane 3CPO$d_3$1 (see figures 3 and 5) and less than three times as viscous as the cyanophenyl-cyclohexane PCH$_5$ [12]. Because of their low viscoelastic ratios (cf. the 22°C data in tables 4 and 6) the new compounds lead to short response times in LCDs. Response times which become still 50 per cent shorter when operating the materials in the first transmission minimum of TN-LCDs, that is, with $d \approx 6\,\mu$m electrode gaps.

5. Electro-optics of TN-LCDs, STN-LCDs, OMI-LCDs and liquid crystal material properties

Whenever new liquid crystals are developed, the question arises as to what extent their material properties will affect the performance of LCDs. In this context the degree to which an electro-optical effect can be multiplexed [21] with a given material is crucial for the quality of the material and the display. Because the new alkenyls will be used mainly in rapidly responding TFT, addressed TN-LCDs as well as in highly multiplexed STN, and OMI-LCDs those liquid crystal material parameters are of special interest that affect these electro-optical effects the most.

The maximum number N of multiplexed lines of an LCD is determined by [21]

$$N = \frac{[(p+1)^2+1]^2}{[(p+1)^2-1]^2} \quad \text{with} \quad p = \frac{V_{50}-V_{10}}{V_{10}}, \tag{5}$$

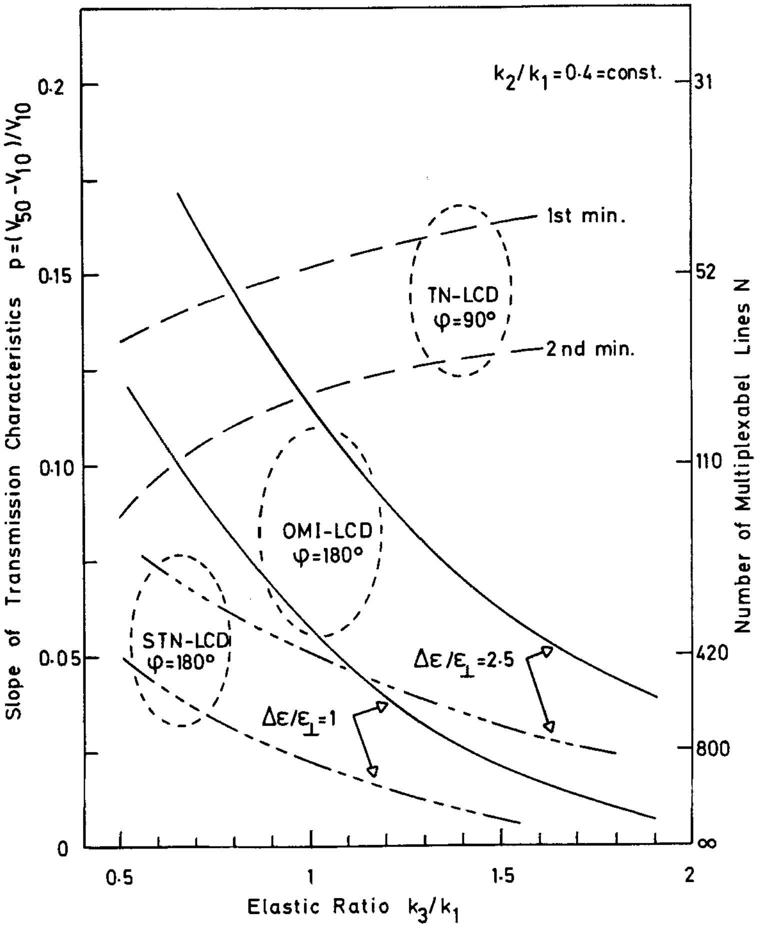

Figure 6. Calculated dependence between the slope parameter p of TN-LCDs, STN-LCDs, OMI-LCDs and the liquid crystal material parameters k_3/k_1 and $\Delta\varepsilon/\varepsilon_\perp$. For TN-LCDs p corresponds to white light which is incident 10° off-axis, whereas for OMI- and STN-LCDs vertical light incidence holds. The following parameters were used: twist angle $\varphi = 180°$ for STN- and OMI-LCDs; $\varphi = 90°$ for TN-LCDs; $\Delta n d$ (STN) = 0·95 μm and $\Delta n d$ (OMI) = 0·50 μm; $k_2/k_1 = 0{\cdot}4$ = constant.

where p is the slope parameter of the transmission voltage characteristics of the LCD. In this definition chosen for p the LCD contrast is 5 : 1. From equation (5) it follows that infinitely steep characteristics result for $p = 0$, that is, $N(p = 0) = \infty$. Figure 6 shows the numerically calculated slope parameters p [5, 6, 22] for TN-LCDs [2], STN-LCDs [4] and OMI-LCDs [5] versus the splay/bend elastic ratio k_3/k_1 and versus $\Delta\varepsilon/\varepsilon_\perp$. Figure 6 illustrates the necessity for a wide range of liquid crystal material properties: whereas low k_3/k_1 ratios are required for TN-LCDs to achieve steep characteristics, the opposite is true for STN- and OMI-LCDs. Moreover, figure 6 shows the strong reduction of multiplexability (which is accompanied by an increase of gray scale capability) when operating TN-LCDs not in their second but in the first transmission minimum [3]. From this and from figure 6 it also follows that alkenyls with odd double bond positions and therefore large k_3/k_1 ratios are specially suited for STN- and OMI-LCDs (cf. k_3/k_1 of 1d_3CC in table 3 or of **M8** in table 5). Thus, rapidly responding, rather low threshold mixtures with elastic ratios of k_3/k_1 = 1·5–2·5 are realistic. They lead in STN-LCDs as well as in OMI-LCDs to virtually infinitely steep characteristics already at moderately low twist angles $\varphi = 180°$ (see figure 6).

6. The overall conformation of ensembles of liquid crystal molecules and the elastic ratio k_{33}/k_{11}

The striking dependence, especially of the elastic ratio k_3/k_1 on the double bond position in alkenyl liquid crystals has already led us [11] to investigate whether rod-like and strain-free molecular conformations exist whose length/width ratios change upon shifting the double bond. The semiquantitative investigations were made with the Roche interactive molecular graphics (RIMG) computer system [23]. RIMG is designed to determine equilibrium structures and conformations of complex molecules based on inter- and intramolecular van der Waals interactions and conformational torsional potentials. Coulomb interactions are not taken into account. The results led us to conclude that the length/width ratio of individual alkenyl molecules cannot be related to their elastic ratios k_3/k_1 [11]. This conclusion is in agreement with earlier experiments which we performed with a number of saturated side chain liquid crystals [18]. It disagrees with some theoretical approaches which refer to experimental data that are not conclusive because non-comparable molecular rods were compared [24]: namely molecules which belong to very different liquid crystal classes with large, class-specific systematic differences of material properties.

From our earlier results [11] and from these findings the question arose as to whether it would be possible to design ensembles comprising a number of molecules such that shifts in double-bond positions would be reflected in changes of the overall equilibrium configuration of the ensembles following from RIMG. Because of the lack of models that would take account of all the relevant inter- and intramolecular interactions governing the complex equilibrium configuration of an ensemble of liquid crystal molecules, the following results should be interpreted with great caution. A detailed article on some correlations between material properties and likely equilibrium configurations of ensembles of molecules will be published elsewhere [25].

Figure 7 shows the equilibrium configuration that results from RIMG of two, initially exactly antiparallel, cyano-phenylcyclohexane molecules 1d_3CP [11]. The broken lines indicate the strength of the intermolecular interactions. As with single molecules [11], the length/width ratio of the equilibrium configuration in figure 7

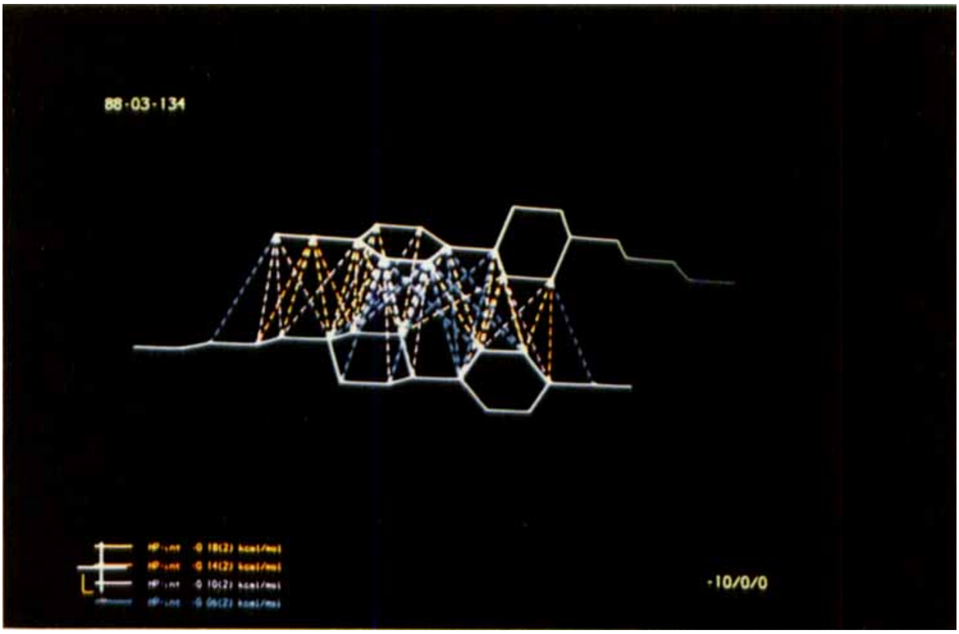

Figure 7. Equilibrium configuration of two antiparallel $1d_3$CP alkenyl molecules following from interactive molecular modelling (RIMG). The broken lines indicate the strength of the intermolecular interactions: brown = strong, red = medium, blue = weak.

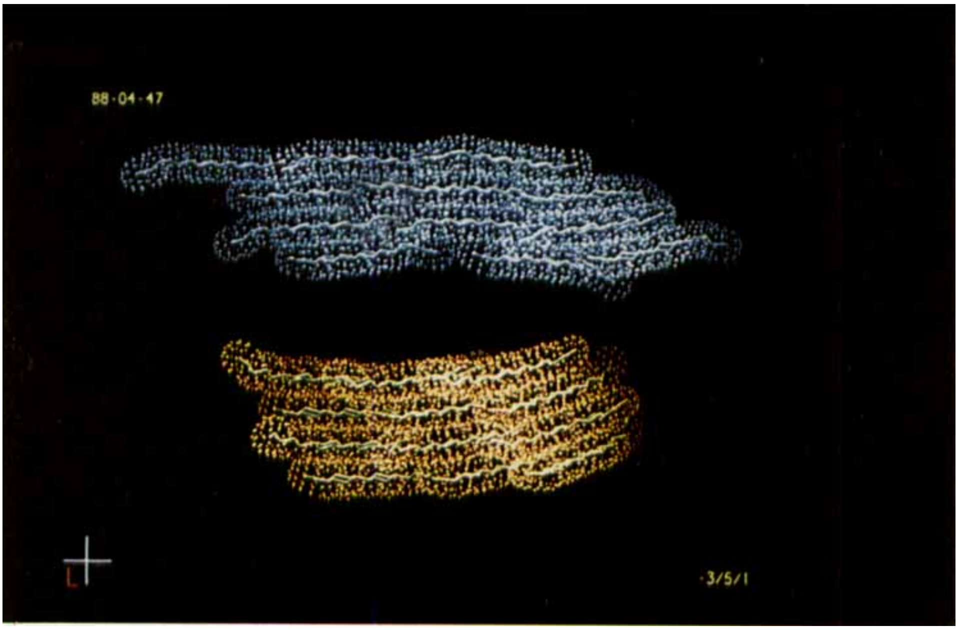

Figure 9. Equilibrium configurations which result from RIMG of ensembles E consisting of $1d_3$CC (blue) and $0d_4$CC (orange) alkenyls. Each ensemble E comprises 12 molecules.

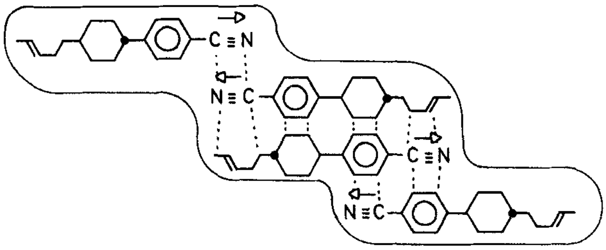

Figure 8. Configuration of a molecular ensemble E_0 before RIMG. The alkenyls shown in the example are of the phenylcyclohexane type $1d_3CP$ [11]. The dotted lines symbolize the interactions resulting from the differences in overlap.

hardly changes when shifting the double bond into different side chain positions. Therefore, and because macroscopic liquid crystal material properties cannot depend only on the structures of individual molecules but must depend also on the short and long range interactions of a significant number of molecules, the following modelling approach was chosen. A two dimensional ensemble E_0 consisting of four cyano-bicyclohexane molecules of the type $1d_3CC$ (see table 1) was assembled such that: (*a*) the permanent dipole moments cancel: (*b*) a preferred alignment of the long molecular axes exists; and (*c*) the three basic configurations depicted in figure 8 occur repeatedly. From the configuration of E_0 in figure 8 follows that a larger nematic ensemble E which consists of four (or more) ensembles E_0 can easily be assembled without violating (*a*)–(*c*). For our purposes an ensemble E consisting of 12 molecules was used. Its most probable equilibrium configuration was determined by RIMG.

Figure 9 shows the equilibrium configurations of two ensembles E in the *xz* plane. The van der Waals radius of each of the 12 molecules is indicated by dots. The upper ensemble (blue) consists of $1d_3CC$ alkenyls whereas the lower ensemble (orange) consists of $0d_4CC$ (see table 1). It is interesting to see that remarkably different length/width ratios of the ensembles E do indeed result when shifting the double bond from the 3 to the 4 position (see figure 9). Whether or not such conformational changes of ensembles E can be related to all of the variations of k_3/k_1 found for polar and non-polar alkenyls (see tables 3 and 5) remains to be seen. However, to our knowledge this is the first time that at least a semiquantitative example is given which indicates that the elastic ratio k_3/k_1 may indeed be proportional to a steric conformation of nematic molecules. Thus, the relation $k_3/k_1 \propto L/W$ suggested by the hard rod models of Priest [26] and Straley [27], although probably not applicable to single molecules, may be applicable to properly chosen ensembles of nematic molecules.

7. Conclusions

In a number of new polar as well as non-polar bicyclohexane alkenyl liquid crystals with double bonds in selective side chain positions, wide nematic mesophases and high nematic–isotropic transition temperatures are found. These alkenyls combine low optical anisotropy and low viscosity with the possibility to tune their elastic properties over a wide range via selectively positioning their side chain double bonds. From investigations and from correlations of the dielectric, birefringence, viscous, viscoelastic and all three elastic constants with the electro-optical performance of TN-LCDs, STN-LCDs and OMI-LCDs it follows that the wide bandwidth of their material properties renders them applicable in rapidly responding, high information content LCDs.

By shifting the alkenyl double bond from even to odd side chain positions in sterically comparable molecules, there are pronounced odd–even effects, especially of the elastic ratio k_3/k_1. Thus k_3/k_1 increases strongly for odd positions, whereas a decrease results for even positions. Moreover, we found a strong increase of the bend elastic constant with decreasing chain length, as well as a strong reduction of the viscoelastic ratio, especially among the short chain representatives of the homologous series Xd_1CC cyanobicyclohexane alkenyls. This shows that small structural changes, especially when made close to the rigid core, may lead to remarkably different material properties. These may not be neglected when correlating, for instance, molecular shapes with material properties.

The elastic odd–even effects found in polar as well as in non-polar bicyclohexane alkenyls are in line with those that we reported for cyano-phenylcyclohexane alkenyls [12]. The viscoelastic ratios γ_1/κ of the positive dielectric anisotropic alkenyls Yd_xCC were related with the response times of TN-LCDs. From the very low γ_1/κ ratios found for selected non-polar alkenyls Yd_xCCOZ fast response times in field-effect LCDs result when combining them with positive dielectric anisotropic nematics. This relation can be generalized to the viscoelastic ratios of other non-polar nematics and their potential response times in TN-LCDs.

Our lack of success as well as that of others in relating the splay/bend elastic ratio k_3/k_1 to the length/width ratio of single rod-shaped liquid crystal molecules led us to explore the influence of different alkenyl side chains on the overall shape of suitably chosen ensembles of molecules. Possible equilibrium configurations of ensembles which consist of 12 molecules each were determined by the Roche interactive molecular graphics computer system. First results indicate that the elastic odd–even effects of k_3/k_1 found for alkenyls may indeed be related to the different length/width ratios of their ensembles. Thus, for the length/width ratios of ensembles E in figure 9 it follows that L/W [E(1d_3CC)] = 4·3, whereas L/W [E(0d_4CC)] = 2·7. The corresponding splay/bend elastic ratios at (T_{NI} − 10°C) are 2·1 and 1·2, respectively (see table 3). We shall explore this approach further which hopefully will lead eventually to quantitative correlations between molecular structural elements and elastic properties of liquid crystals.

We gratefully acknowledge the experimental assistance of B. Blöchliger, A. Germann and J. Reichhardt.

References

[1] Morozumi, S., Oguchi, K., Misawa, T., Araki, R., and Oshima, H., 1984, *Dig. SID*, 316.

[2] Schadt, M., and Helfrich, W., 1971, *Appl. Phys. Lett.*, **18**, 127.

[3] Baur, G., 1981, *Molec. Crystals liq. Crystals*, **63**, 45.

[4] Kando, Y., Nakagomi, T., and Hasagewa, S., 1985, German Offenlegungsschrift DE 3503259 A1.

[5] Schadt, M., and Leenhouts, F., 1987, *Appl. Phys. Lett.*, **50**, 236; 1987, *Proc. SID*, **29**, 375.

[6] Leenhouts, F., and Schadt, M., 1986, *SID Proc. Japan Display '86*, 388.

[7] Osman, M. A., and Révész, L., 1979, *Molec. Crystals liq. Crystals*, **56**, 105.

[8] Eidenschink, R., Erdmann, D., Krause, J., and Pohl, L., 1978, *Angew. Chem.*, **90**, 133.

[9] Eidenschink, R., Römer, M., Weber, G., Gray, G., and Johnson, T. K., 1984, German Offenlegungsschrift DE 3321373 A1.

[10] Praefke, K., Schmidt, D., and Heppke, G., 1980, *Chem. Z.*, **104**, 269.

[11] Schadt, M., Petrzilka, M., Gerber, P. R., and Villiger, A., 1985, *Molec. Crystals liq. Crystals*, **122**, 241.

[12] Schadt, M., Buchecker, R., Leenhouts, F., Boller, A., Villiger, A., and Petrzilka, M., 1986, *Molec. Crystals liq. Crystals*, **139**, 1.
[13] Buchecker, R., and Schadt, M., 1987, *Molec. Crystals, liq. Crystals*, **149**, 359.
[14] Schadt, M., and Müller, F., 1978, *I.E.E.E. Trans. electron. Devices*, **15**, 1125; 1981, *Molec. Crystals liq. Crystals*, **65**, 241.
[15] Janning, J. L., 1972, *Appl. Phys. Lett.*, **21**, 173.
[16] Gerber, P. R., and Schadt, M., 1980, *Z. Naturf. (a)*, **35**, 1036.
[17] Gruler, H., and Cheung, L., 1975, *J. appl. Phys.*, **46**, 5097.
[18a] Gerber, P. R., 1981, *Appl. Phys.* A, **26**, 139.
[18] Schadt, M., and Gerber, P. R., 1982, *Z. Naturf. (a)*, **37**, 165.
[19] de Jeu, H. W., and Classen, W. A. P., 1977, *J. chem. Phys.*, **67**, 3705.
[20] Jakeman, E., and Raynes, E. P., 1972, *Phys. Lett.* A, **39**, 69.
[21] Alt, P. M., and Pleshko, P., 1974, *I.E.E.E. Trans. electron. Devices*, **21**, 146.
[22] Schadt, M., Buchecker, R., Villiger, A., Leenhouts, F., and Fromm, J., 1986, *I.E.E.E. Trans. electron. Devices*, **33**, 1187.
[23] Müller, K., Ammann, H. J., Doran, D. M., Gerber, P., and Schrepfer, G., 1986, *Innovative Approaches in Drug Research* (Elsevier Science), pp. 125–134.
[24] Govers, E., and Vertogen, G., 1987, *Liq. Crystals*, **2**, 31.
[25] Schadt, M., and Müller, K., (to be published).
[26] Priest, R. G., 1973, *Phys. Rev.* A, **7**, 720.
[27] Straley, J. P., 1973, *Phys. Rev.* A, **8**, 2181.